Zoological Journal of the Linnean Society, 2020, **XX**, 1–20. With 6 figures.

Molecular phylogeny and morphological diversity of the *Niviventer fulvescens* species complex with emphasis on species from China

DEYAN GE[1†], ANDERSON FEIJÓ[1†], ALEXEI V. ABRAMOV[2], ZHIXIN WEN[1], ZHENGJIA LIU[3], JILONG CHENG[1], LIN XIA[1], LIANG LU[4*] and QISEN YANG[1*]

[1]*Key Laboratory of Zoological Systematics and Evolution, Institute of Zoology, Chinese Academy of Sciences, Beichen West Road, Chaoyang District, Beijing 100101, China*
[2]*Zoological Institute, Russian Academy of Sciences, Saint Petersburg 199034, Russia; Joint Russian–Vietnamese Tropical Research and Technological Centre, Hanoi, Vietnam*
[3]*Institute of Geographic Sciences and Natural Resources Research, Chinese Academy of Sciences, Beichen West Road, Chaoyang District, Beijing, 100101, China*
[4]*State Key Laboratory for Infectious Diseases Prevention and Control, National Institute for Communicable Disease Control and Prevention, Chinese Center for Disease Control and Prevention, Beijing, 102206, China*

Received 28 August 2019; revised 5 March 2020; accepted for publication 25 March 2020

The *Niviventer fulvescens* species complex (NFSC), a group of abundant and taxonomically ambiguous rodent taxa, is distributed from Southeast Asia to south-eastern China. We combined molecular and morphological datasets to clarify the species composition and variation of the NFSC. Our phylogenetic analyses, using molecular data, recovered eight genetic lineages in the NFSC, including a novel, distinct lineage from Jilong, Tibet, China, which is described as a new species**, *N. fengi* sp. nov.** The species status of *N. fengi* is supported by a species delimitation analysis, and it is morphologically distinguished from other members of the NFSC by its greyish dorsal fur, soft hairs covering the whole body and a hairy tail. NFSC species bearing well-developed spines are found at lower elevations. A comprehensive taxonomic revision of the NFSC within China is provided, represented by five species: *N. cremoriventer*, *N. fulvescens*, *N. huang*, ***N. mekongis* comb. nov.** and *N. fengi*. A further study of this species complex, including samples from Southeast Asia, is needed.

ADDITIONAL KEYWORDS: mammals – molecular phylogeny – morphological comparison – Murinae – new species – rats – rodents.

INTRODUCTION

The white-bellied rats (*Niviventer* Marshall, 1976) belong to the most common rat taxon distributed from South and Southeast Asia to northern China. They are abundant in natural forests and occupy lowlands to high-elevation mountains. These species are omnivorous and are active on the ground or on tree trunks at night. Four species complexes, namely, the *N. andersoni* species complex (NASC), *N. niviventer* species complex (NNSC), *N. eha* species complex (NESC) and the *N. fulvescens* species complex (NFSC), were recognized in previous studies (Balakirev *et al.*, 2011, 2014; He & Jiang, 2015; Lu *et al.*, 2015; Zhang *et al.*, 2016).

The NASC and NESC inhabit middle to high elevations in forests, while the NNSC and NFSC occupy a wider elevational range. Species of the NASC [*N. andersoni* (Thomas, 1911) and *N. excelsior* (Thomas, 1911)] and NESC [*N. brahma* (Thomas, 1914) and *N. eha* (Wroughton, 1916)] are easily identified based on their external morphology. The NASC can be

*Corresponding authors. Email: luliang@icdc.com.cn; yangqs@ioz.ac.cn
†Contributed equally to the present study.
[Version of record, published online 13 May 2020; http://zoobank.org/ urn:lsid:zoobank.org:pub: A0C63287-87B3-42E0-BC0E-CACDE62A8137]

distinguished from the NESC by a larger size and pure-white belly, while the ventral fur of the NESC members is greyish white. Ge *et al.*, (2018) recognized eight NNSC species in China. However, the NFSC continues to present longstanding taxonomic controversies. The NFSC was assigned to the '*Rattus huang–fulvescens* group' by Tate (1936) or the '*cremoriventer* group' and '*confucianus–huang* group' by Ellerman (1940). Musser (1981) listed 15 taxa as synonyms of *N. fulvescens* (Gray, 1847) [*N. blythi* (Kloss, 1917), *N. blythi mekongis* Robinson & Kloss, 1922, *N. caudatior* (Hodgson, 1849), *N. cinnamomeus* (Blyth, 1844), *N. flavipilis* (Shih, 1930), *N. gracilis* (Miller, 1913), *N. huang* (Bonhote, 1905), *N. jerdoni* (Blyth, 1863), *N. lepidus* (Miller, 1913), *N. ling* (Bonhote, 1905), *N. minor* (Shih, 1930), *N. octomammis* (Gray, 1863), *N. orbus* (Robinson & Kloss, 1914), *N. vulpicolor* (Allen, 1926) and *N. wongi* (Shih, 1931)] and placed them in 'the *Niviventer* complex'. Members of this complex are recognized as spiny-haired rats and are easily misidentified as members of the NNSC in the field.

Osgood (1932) distinguished *N. confucianus* (Milne-Edwards, 1871) from *N. fulvescens* on the basis of the larger size, darker colour, frequently white-tipped tail, frequently fulvous-marked breast, larger and more globose auditory bullae, and longer and more compressed nasals of the former (Musser, 1981). Stefen & Rudolf (2007) summarized major features that distinguished the NFSC and NNSC, including the brighter, more reddish ochraceous pelage of *N. fulvescens*, the width of the interorbital region, the length of the incisive foramen, the anterior rim of the zygomatic plate, and traits of the mandible and maxillary teeth. However, criteria for distinguishing species within the NFSC were not addressed in previous studies. In China, members of this complex are generally considered to be a single species, *N. fulvescens* (Smith & Xie, 2008), but recent studies have revealed that species diversity within the NFSC is underestimated, based on both molecular and morphological data (Balakirev *et al.*, 2011, 2014; He & Jiang, 2015; Lu *et al.*, 2015; Zhang *et al.*, 2016; Ge *et al.*, 2018).

Previous studies have highlighted the monophyletic position of the NFSC and placed it as either sister to all other members of the genus *Niviventer* or as the sister group of the NESC (Balakirev *et al.*, 2011, 2014; He & Jiang, 2015; Lu *et al.*, 2015; Zhang *et al.*, 2016; Ge *et al.*, 2018). According to external morphology, the NFSC probably includes *N. cameroni* (Chasen, 1940), *N. cremoriventer* (Miller, 1900), *N. fraternus* (Robinson & Kloss, 1916), *N. fulvescens*, *N. huang*, *N. lepturus* (Jentink, 1879), *N. hinpoon* (Marshall, 1976) and *N. rapit* (Bonhote, 1903). Among these species, *N. cameroni* is endemic to the Cameron Highlands, Peninsular Malaysia, *N. fraternus* is endemic to western Sumatra, *N. rapit* is restricted to Borneo and *N. lepturus* is only found in western and central Java (Musser & Carleton, 2005; Denys *et al.*, 2017). These species are easily distinguished from other members of the NFSC because they are morphologically distinct and do not geographically overlap. The remaining species of the NFSC occur from Southeast Asia to central China and appear to be among the most taxonomically ambiguous taxa of murids, because no comprehensive morphological, molecular and biogeographical studies have been conducted.

We here aim to clarify the taxonomy of the NFSC in China by integrating morphological and molecular datasets. Based on molecular data, one novel genetic lineage from Jilong, Tibet, was discovered in the present study. A comprehensive taxonomic revision of the NFSC in China and a description of this new lineage are provided in the taxonomic account.

MATERIAL AND METHODS

Molecular sampling and sequencing

Specimens of *Niviventer* were collected by our team and deposited at the Institute of Zoology, Chinese Academy of Sciences, Beijing, China (IOZCAS), the National Institute for Communicable Disease Control and Prevention, Beijing, China (ICDC) and the Zoological Institute of the Russian Academy of Sciences, Saint Petersburg, Russia (ZIN). In total, we used 300 metal pedal traps per day with peanut seeds as bait and performed sampling during eight continuous nights. Total genomic DNA was isolated from muscle or liver tissue using a Qiagen DNeasy blood and tissue kit (Qiagen China, Pudong, Shanghai, China). The primer sequences used for PCR and sequencing, and their original references, were the same as those used in previous studies (Ge *et al.*, 2018, 2019). PCR products were directly sequenced in both directions with an ABI 3100 automatic sequencer (Perkin-Elmer, Waltham, Massachusetts) using an ABI PRISM BigDye Terminator Cycle Sequencing Ready Reaction Kit with AmpliTaq DNA polymerase (Applied Biosystems, Foster City, California). Among approximately 1000 newly sequenced samples, 151 were assigned to the NFSC in preliminary phylogenetic analyses (Supporting Information, Table S1).

Phylogenetic reconstruction

We compiled three datasets for the phylogenetic analyses. In the first dataset, we supplemented newly sequenced cytochrome *b* (*Cytb*) sequences with sequences from previous studies: a total of 894

individuals were included in the analyses (Jing *et al.*, 2007; Balakirev *et al.*, 2011, 2014; Lu *et al.*, 2015; Zhang *et al.*, 2016; Ge *et al.*, 2018). In the second dataset, we supplemented sequences of *Cytb*, cytochrome *b* oxidase subunit I (*COI*) and D-loop with sequences from previous studies (Lu *et al.*, 2015; Ge *et al.*, 2018, 2019) to establish a concatenated dataset of three mitochondrial DNA (mtDNA) fragments from 366 individuals. Samples with all three fragments were used in the analyses. In the third dataset, newly sequenced interphotoreceptor retinoid binding protein (*Rbp3*) sequences were combined with the results of previous studies to test phylogenetic differentiation based on nuclear data. Detailed information on the samples and GenBank accessions of the DNA sequences are provided in Supporting Information, Table S1 and the locations of the samples are shown in Fig. 1. *Apodemus draco* (Barrett-Hamilton, 1900), *A. flavicollis* (Melchior, 1834), *Bandicota indica* (Bechstein, 1800), *Berylmys berdmorei* (Blyth, 1851), *Chiromyscus* sp., *Leopoldamys sabanus* (Thomas, 1887), *Mus musculus* Linnaeus, 1758 and *Rattus norvegicus* Linnaeus, 1758 were used as outgroups in both datasets.

Sequences were aligned using MUSCLE v.3.8.81 (Edgar, 2004) in MEGA X (Kumar *et al.*, 2018). To reduce computational demand and over-partitioning, we used DAMBE v.5.5.29 (Xia, 2013) to delete duplicated sequences and PartitionFinder 2 (Lanfear *et al.*, 2017) to select the best-fitting nucleotide substitution model settings for *Cytb* (1131 bp), *COI* (676 bp), *Rbp3* (1194) and the whole D-loop fragment (564 bp). We conducted Bayesian phylogenetic analyses (BP) of the three datasets using the parallel version of MrBayes v.3.1.2 (Ronquist *et al.*, 2012). We performed four independent runs of each dataset, with two cold and two heated Markov chains of 80 million steps. Trees were sampled every 1000 steps and the first 25% were discarded as burn-in. Convergence was monitored using the standard deviation of split frequencies, and we monitored for sufficient sampling using TRACER (Rambaut & Drummond, 2007). Additionally, we

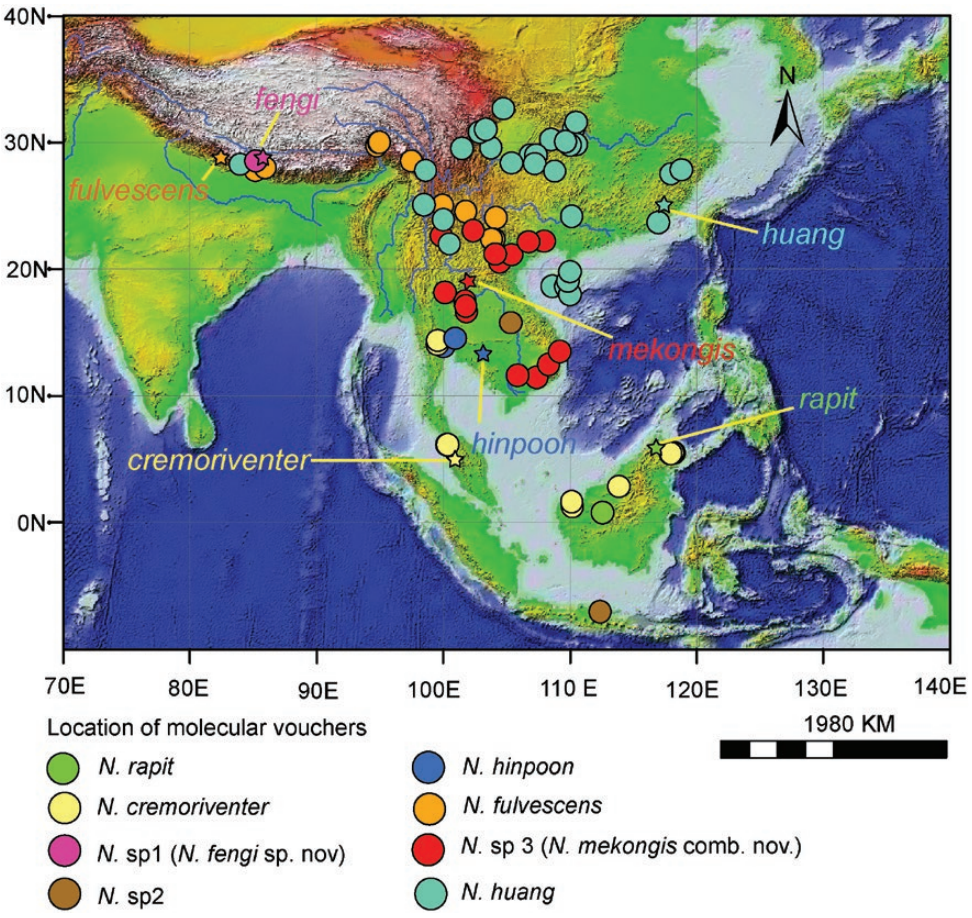

Figure 1. Distribution of molecular voucher specimens showing the spatial partitions between species within the NFSC. The holotype localities of the taxa studied in the present work are indicated on the map using colours corresponding to the molecular voucher specimens.

performed maximum likelihood (ML) analyses of these datasets in IQ-TREE v.1.6.12 (Nguyen *et al.*, 2015) with 1000 ultrafast bootstraps and 1000 replicates using SH-like approximate likelihood ratio test for branches supports. Substitution models of each data partitions were tested automatically during analyses.

Sequence divergence between or within species was calculated as the uncorrected p-distance based on *Cytb* and *COI* sequences in MEGA X, because these two fragments are the most frequently used DNA markers for calculating genetic distance between sister-taxa in mammals.

Species delimitation using molecular data

We employed three different models to delimit species within the NFSC by using molecular data: the generalized mixed Yule coalescent in the R splits package (Fujisawa & Barraclough, 2013) under the more reliable single-threshold model, which is a likelihood method for delimiting species by fitting within- and between-species branching models to reconstructed gene trees (GMYC; Kapli *et al.*, 2017); Poisson tree processes (PTP; Zhang *et al.*, 2013), which infer putative species boundaries on the basis of a given phylogenetic input tree; and multi-rate Poisson tree processes (MPTP; Kapli *et al.*, 2017), which is an improved method that alleviates the theoretical and technical shortcomings of PTP. We used the default parameters of the last two models in the analyses. The Bayesian tree obtained using the concatenated dataset of three mitochondrion DNA fragments from the above analyses was employed in further analyses. The NNSC, NASC, NESC and outgroup taxa were removed in the analyses. The clusters identified by GMYC, PTP and MPTP were considered as the optimal taxonomic units (OTU) in the NFSC.

Testing for morphological variation

We examined the NFSC specimens that were preserved in the following museums: the Natural History Museum, London, United Kingdom (NHM); the Kunming Institute of Zoology of the Chinese Academy of Sciences, Kunming, China (KMIOZCAS); Marine College, Shandong University, Shandong, China (MCSU); Zoological Museum of the Moscow State University, Moscow, Russia (ZMMU); Field Museum of Natural History, Chicago, United States of America (FMNH); ZIN; IDDC and IOZCAS.

Regarding general morphology, we compared fur coloration and rigidity between different lineages by photographing specimens of adult individuals and intact pelages. The presence or absence of spines and the seasonal variation of skin coloration were recorded. Body mass (BM, g) and four external measurements (EMs, mm), including head and body length (HBL), tail length (TL), ear length (EL) and hindfoot length (HFL, excluding the claw), were included in the analyses. We calculated the mean and standard deviation of the EMs for each species. Pairwise differences in the BM, HBL, TL, HFL and EL between species were tested by an analysis of variance (ANOVA) using least significant difference (LSD) tests. A list of 205 specimens examined for the assessment of general morphology, including their museum collection numbers and original measurements, is given in Supporting Information, Table S2.

Quantitative craniodental characters comprising 16 measurements were taken with digital callipers to the nearest 0.01 mm from 124 adult specimens of both sexes following the criteria described by Ge *et al.*, (2018). These craniodental measurements (CMs) were as follows: total length of the cranium (TLC), nasal length (NL), greatest width of the 'snout' (GWS), shortest distance between orbits (SDO), zygomatic breadth (ZB), greatest mastoid breadth (GMB), palatal length (PL), incisive foramen length (IFL), width of the incisive foramen (WIF), greatest palatal breadth (GPB), length of the tympanic bulla (LTB), length of the maxillary molars (ULMM), length of the maxillary diastema (ULMD), mandibular length (ML), length of the mandibular molars (LLMM) and length of the mandibular diastema (LLMD). The locations of these measurements are provided in Supporting Information, Fig. S1 and the original values of the CMs for 124 specimens are given in Supporting Information, Table S3.

Principal component analysis (PCA) was performed on the correlation matrix of the $\log_{10}$-transformed CMs and used as an exploratory tool for investigating the major patterns of variation and evaluating the degree of separation among members of the NFSC. Multivariate ANOVAs (MANOVAs) of the PCA scores were conducted. We used linear discriminant analyses (LDAs) to test group membership based on the taxonomy revealed by our molecular phylogenetic reconstruction, with or without leave-one-out cross-validation for comparison. We tested the significance of the morphological differences between species by using MANOVA of discriminant scores. All statistical analyses were conducted in PAST 3.16 (Hammer *et al.*, 2001) and in R software (R Core Team, 2017).

RESULTS

Molecular phylogeny and taxonomic assignment

Both *Cytb* and the concatenated dataset of three mtDNA fragments recover well-supported monophyletic

clades within the NFSC by BP and ML (Figs 2, 3). Phylogenetic analyses based on *Cytb* recover eight genetic clades within the NFSC, which were assigned to *N. rapit*, *N. cremoriventer*, *N. fulvescens*, *N. huang*, *N.* sp. 1, *N.* sp. 2 and *N.* sp. 3, numbered 1–7 in Figure 2. It should be mentioned that a large number of voucher specimens with data in GenBank were misidentified in their original publication. For example, KY117572, identified as *N. cremoriventer* by Mohd Salleh *et al.*, (2017), clusters with DQ191483 and HQ877098 (both from voucher specimen UMMZ174435), which were assigned to *N. rapit* in their respective original

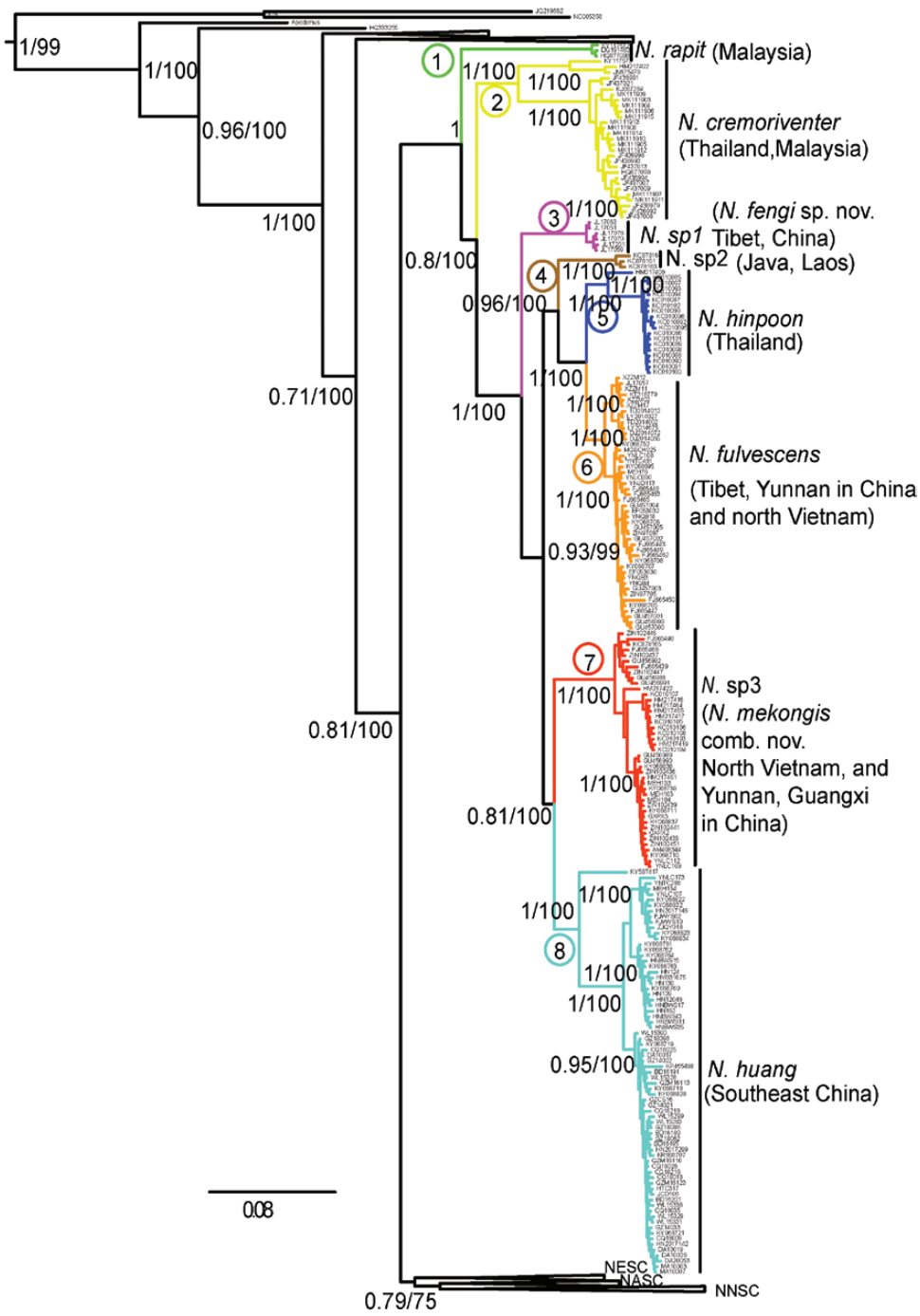

Figure 2. Phylogeny of the NFSC reconstructed by using *Cytb*. Posterior probabilities from Bayesian analyses in MrBayes and bootstrap values from maximum likelihood analyses in IQ-TREE are given as node labels.

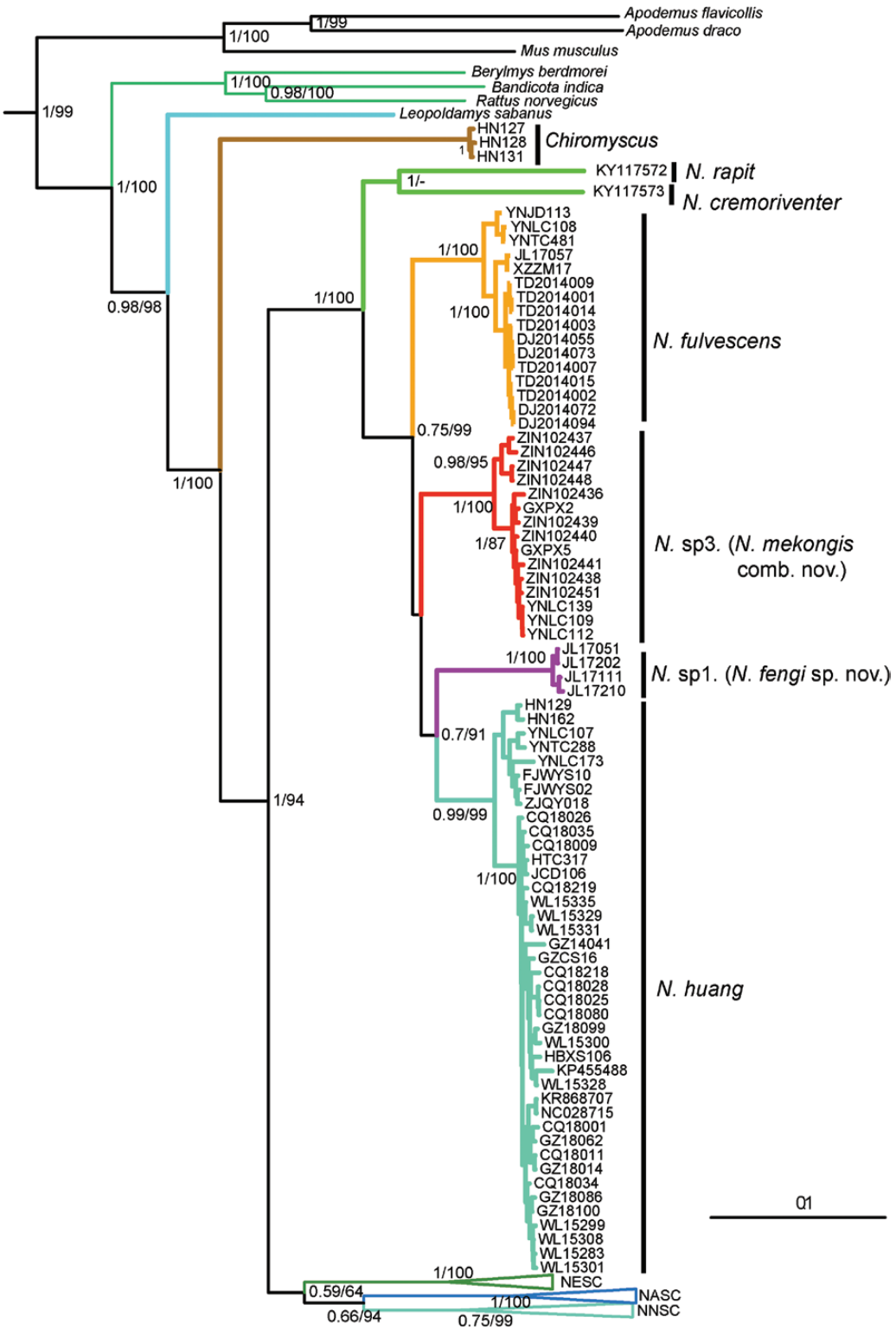

Figure 3. Phylogeny of the NFSC reconstructed by using the concatenated dataset of three mitochondrial DNA fragments. Posterior probabilities from Bayesian analyses in MrBayes and bootstrap values from maximum likelihood analyses in IQ-TREE are given as node labels.

publications (Gorog *et al.*, 2004; Jansa *et al.*, 2006). This specimen was collected from Bukit Baka-Bukit Raya National Park, Borneo, Indonesia, not too far from the type locality of *N. rapit* (Sabah, N Borneo, Gunung Kinabalu, Malaysia). We assigned this genetic lineage to *N. rapit*. The tail of *N. rapit* is clearly longer than that of sympatric *N. cremoriventer*.

A large number of sequences cluster into the second genetic lineage, most of which were assigned to *N. cremoriventer* in original publications (Aplin *et al.*, 2011; Brunke *et al.*, 2019). We accepted this idea by assigning this lineage as *N. cremoriventer*. The samples of this lineage were collected from Borneo, Kedah in Malaysia, Regu, Padawan in Malaysia and Kanchanaburi in Thailand. The second locality is near the type locality of *N. cremoriventer*.

Samples comprising the third genetic lineage were collected from Jilong Valley, Jilong County, Shigatse, Tibet, China. The morphology of this lineage is markedly different from that of other species within the NFSC (see detailed information below). Here, we temporarily assign the lineage to *N.* sp. 1 (we give it the new name *N. fengi*, the description below).

The fourth lineage, including KC878161, KC878163 and KC878164, collected from west Java and Khammouane, Laos, was assigned to *N. bukit* in the study by Achmadi *et al.,* (2013). Recent studies have placed *N. bukit* in the NNSC (Balakirev *et al.*, 2014; Lu *et al.*, 2015; Ge *et al.,* 2018). The voucher specimen of KC878164, WAM-M38541, in the Western Australian Museum, was assigned to *N. fulvescens* by Pahl *et al.,* (2018), which is consistent with its placement within the NFSC in the present study. However, the species assignment of this genetic lineage (*N.* sp. 2) is pending, because no voucher specimens were available for the present study.

The fifth lineage includes HM217409 and KC010085-KC010102 from Kanchanaburi (near the type locality of *N. hinpoon*, Saraburi Province, Kaengkhoi District), Thailand, which were assigned to *N. hinpoon* by Latinne *et al.,* (2013). We agree with this assignment.

The sixth lineage, *N. fulvescens*, is the sister lineage of *N. hinpoon*, mainly from high- to medium-elevation mountains in south-western Yunnan and south-eastern Tibet. Some of these samples were collected close to the type locality of *N. fulvescens*.

The seventh lineage, including samples from Vietnam and Yunnan and Guangxi Provinces in China, was previously assigned to *N. huang* (Balakirev *et al.*, 2011, 2014; Lu *et al.*, 2015), but the type locality of *N. huang* is in Kuatun, Fujian Province, China. Here, we assign this lineage to *N.* sp. 3 (it can be treated as ***N. mekongis* comb. nov.**, see description below).

A large number of samples from south-east China, including samples from Yunnan, Fujian, Zhejiang, Hunan, Guizhou, Hubei, Chong Qing, Sichuan and Hainan, form the eighth lineage, which we designate as the true *N. huang*.

The phylogeny reconstructed by using the concatenated dataset of three mtDNA fragments is similar to that reconstructed with *Cytb* alone, which placed *N. rapit* as sister to the rest of the NFSC (Fig. 3). The split among *N. fulvescens*, *N.* sp. 1, *N.* sp. 3 and *N. huang* likely occurred rapidly since the internal branches were not well supported, despite recovery of the monophyly of each lineage. The BP and ML trees of *Rbp3* reveal *N.* sp. 1 to be a highly supported monophyletic clade, while *N.* sp. 3 and *N. huang* appear to be paraphyletic (Supporting Information, Fig. S2).

The genetic distance between species ranges from 0.125 ± 0.02 to 0.080 ± 0.01 based on *Cytb* and from 0.11 ± 0.02 to 0.052 ± 0.01 based on *COI* (Table 1).

OTUs identified via species delimitation

GMYC identified six OTUs using the tree reconstructed based on the concatenated dataset of three mitochondrial DNA fragments. PTP identified 14 OTUs from the same tree, while MPTP identified 11 OTUs. All methods used for species delimitation recognized *N. rapit*, *N. cremoriventer*, *N. fulvescens*, *N. huang*, *N.* sp. 1 and *N.* sp. 3 as independent OTUs. The result of GMYC was consistent with the

Table 1. Genetic distance calculated based on molecular data. Estimates of evolutionary divergence (with standard errors) across species pairs using *Cytb* are given in the lower triangle, and those obtained using *COI* are given in the upper triangle; within-species distances using *Cytb* are given on the diagonal. Abbreviations for species: NC, *N. cremoriventer*; NF, *N. fulvescens*; NH, *N. huang*; NM, *N. mekongis*; NFE, *N. fengi*

	NC	NF	NH	NM	NFE
NC	0.090 ± 0.012	0.102 ± 0.017	0.102 ± 0.016	0.108 ± 0.018	0.113 ± 0.018
NF	0.1171 ± 0.0118	0.013 ± 0.002	0.060 ± 0.011	0.059 ± 0.012	0.056 ± 0.011
NH	0.1189 ± 0.0146	0.0865 ± 0.0120	0.012 ± 0.002	0.052 ± 0.01	0.062 ± 0.012
NM	0.1252 ± 0.0159	0.0793 ± 0.0118	0.0803 ± 0.0109	0.012 ± 0.002	0.066 ± 0.012
NFE	0.1137 ± 0.0141	0.0873 ± 0.0130	0.0841 ± 0.0116	0.0903 ± 0.0125	0.004 ± 0.001

systematics established based on morphology, while PTP and MPTP likely overestimated the number of OTUs. However, oversplitting is a common problem for PTP and MPTP when a greater number of species are involved in the analyses (Luo *et al.*, 2018). A comparison of these results is presented in Supporting Information, Fig. S3.

Morphological comparison across species

Niviventer sp. 1 is the smallest species within the NFSC (Table 2; Figs 4, 5), easily distinguishable from *N. fulvescens*, *N. huang* and *N.* sp. 3 (Table 2; Figs 4, 5) based on EMs and CMs (Table 3; Figs 4, 5). It also exhibits soft hairs over its entire body and greyish black coloration in dorsal view, which is a distinct overall fur trait within the NFSC (Fig. 6). Pairwise comparisons revealed that most species pairs were distinct based on EMs ($P < 0.05$), except for *N. cremoriventer* and *N. fulvescens* (BM, $P = 0.436$; HBL, $P = 0.749$; TL, $P = 0.069$; HFL, $P = 0.464$; EL, $P = 0.228$). MANOVA of CMs revealed significant morphological differences among species ($P < 0.001$). The first PC (PC1) of the CMs explained 48.2% of the overall variation, while the second PC (PC2) explained 10.8% (Supporting Information, Table S4). The PC plot shows considerable overlap among species, but *N.* sp. 1 is clearly differentiated from *N. cremoriventer* and *N.* sp. 3 (Fig. 4A). The overall correct classification percentage of the cross-validated discriminant analysis is 65% with jackknife estimation, but 80% without jackknife estimation. *Niviventer* sp. 3, *N. huang* and *N. cremoriventer* have the highest rates of correct classification. A plot of the first and second discriminant functions shows clear separation of *N.* sp. 3 and *N.* sp. 1 from all other species (Fig. 4B). *Niviventer cremoriventer and N. huang* are also differentiated along the DF1 axis.

DISCUSSION

Morphological variation in the NFSC

Previous studies showed that qualitative aspects of the cranium had only limited value in distinguishing species of the NFSC (Musser, 1973; Balakirev *et al.*, 2011). Here, we find that most of the morphological differences among NFSC species are in overall external morphology, fur colour, spine presence and morphology, foot colour and tail morphology, which can be easily assessed in the field (see Taxonomic account section below). In addition, some of the EMs and CMs also show significant differences between species and can thus be used to confirm their identities (Tables 2, 3; Fig. 4).

According to Gloger's rule, animal coloration is linked to climatic variation, particularly variation in temperature and humidity. For example, birds and mammals tend to be more pigmented in tropical regions (Rensch 1929; Delhey 2019). Taking *Micromys* as an example: *M. minutus*, which is widely distributed in northern Asia and Europe, exhibits light brown dorsal coloration, while *M. erythrotis*, from northern Vietnam and southern China, exhibits dark brown dorsal coloration (Abramov *et al.*, 2009). This is also the case in the genus *Niviventer*, which shows an increase in pigmentation with higher temperatures in tropical regions, but reduced pigmentation in northern regions. For example, the dorsal coloration of *N. confucianus* changes from dark brown to greyish brown from south to north in China (see fig. 8 in Ge *et al.*, 2018). Species of *Niviventer* typical of low elevations (higher temperatures and humidity) tend to have a bright fulvous colour (e.g. *N.* sp. 3 and *N. huang*), whereas those associated with high elevations tend to have a darker colour (e.g. *N.* sp. 1 and *N. eha*).

Another interesting aspect of the morphological evolution of *Niviventer* is the presence of spines, which occur in multiple species of this genus. Hairs and hair-related integumentary structures are fundamental to the livelihood of mammals (Martin *et al.*, 2015). Additionally, spines seem to have thermoregulatory and water condensation functions in tropical and subtropical rodent species (Goncalves *et al.*, 2018). Previous studies considered the presence of spines an important character in the taxonomy of *N. fulvescens* (Smith & Xie, 2008). Notably, species bearing only soft hairs, e.g. *N. brahma*, *N. eha*, *N. excelsior*, *N. pianmaensis* and *N.* sp. 1, are all distributed at higher elevations. In contrast, species bearing well-developed spines, e.g. *N. confucianus*, *N. huang* and *N.* sp. 3, are distributed at lower elevations. The association between soft hairs and high elevations (or spiny hairs and low elevations) in *Niviventer* could be related to numerous factors. For instance, soft hairs could have evolved to cope with cold temperatures at higher elevations or reflect a plastic response to environmental conditions. The genetic mechanisms that drive the differences in the phenotype of hairs in *Niviventer* species, as well as its biological function, deserve further study.

Distribution and diversification of the NFSC

Compared with members of the NNSC, those of the NFSC inhabit a more southern region within the overall distribution range of the genus *Niviventer*. Species within the NFSC showed clear differentiation from Southeast Asia to southern China (Fig. 1). According to the distribution of molecular voucher specimens, *N. huang* occupies a large area in south-eastern China with an average elevation of ~1300

Table 2. External and craniodental measurements (mean ± 1 SD, range; in mm) of NFSC members in China. The abbreviations for the species are the same as in Table 1. BM, body mass (g); EMs, external measurements; HBL, head and body length; TL, tail length; HFL, hind foot length; EL, ear length; CMs, craniodental measurements; TLC, total length of the cranium; NL, nasal length; GWS, greatest width of the 'snout'; SDO, shortest distance between orbits; ZB, zygomatic breadth; GMB, greatest mastoid breadth; PL, palatal length; IFL, incisive foramen length; WIF, width of the incisive foramen; GPB, greatest palatal breadth; LTB, length of the tympanic bulla; ULMM, length of the maxillary molars; ULMD, length of the maxillary diastema; ML, mandibular length; N, number of specimens examined; LLMM, length of the mandibular molars; LLMD, length of the mandibular diastema

	NC	**NF**	**NH**	**NFE**	**NM**
EMs	*N* = 10	*N* = 37	*N* = 105	*N* = 15	*N* = 18
BM	62.1 ± 6.40	66.82 ± 14.04	73.67 ± 17.81	53.67 ± 14.03	78.98 ± 22.49
	51–68	40–91	40.00–120.40	41–80	46.40–126.00
HBL	133 ± 6.04	131.60 ± 1	135.36 ± 12.30	126.47 ± 14.03	139.08 ± 15.37
	125–148	105–160	119–165	110–160	105–163
TL	178.13 ± 14.80	187.74 ± 14.94	172.08 ± 11.84	146.07 ± 14.19	181.18 ± 16.60
	158–201	150–216	140–205	127–180	143–216
HFL	26.80 ± 0.92	27.22 ± 2.01	28.11 ± 1.53	24.93 ± 1.49	28.98 ± 1.62
	26–29	23–31	23–32	22–28	24–31
EL	19.20 ± 1.03	20 ± 2.50	19.64 ± 1.81	19.53 ± 1.46	19.72 ± 1.31
		13–24	10–22	17–22	17–23
CMs	*N* = 29	*N* = 29	*N* = 50	*N* = 9	*N* = 6
TLC	34.67 ± 1.41	35.15 ± 1.73	34.78 ± 2.01	32.44 ± 1.98	37.84 ± 0.70
	31.22–36.94	31.18–39.06	29.35–35.96	29.63–35.96	36.73–38.66
NL	12.31 ± 0.59	12.92 ± 1.22	12.85 ± 1.27	11.49 ± 1.24	14.53 ± 1.22
	10.43–13.33	10.47–15.55	10.77–16.75	9.87–13.82	13.56–16.93
GWS	5.78 ± 0.58	5.40 ± 0.44	5.32 ± 0.41	5.36 ± 0.49	5.64 ± 0.33
	4.51–6.74	4.36–6.23	4.60–6.28	4.60–6.18	5.20–6.12
SDO	5.93 ± 0.25	5.65 ± 0.30	5.65 ± 0.32	5.17 ± 0.28	5.89 ± 0.29
	5.40–6.68	5.16–6.34	4.92–6.39	4.76–5.84	5.60–6.31
ZB	15.50 ± 0.93	15.09 ± 1.24	14.89 ± 1.19	14.84 ± 0.60	16.92 ± 0.63
	13.98–17.14	12.72–17.63	11.63–16.97	14.25–15.97	16.21–17.58
GMB	13.87 ± 0.68	13.28 ± 0.61	13.13 ± 0.60	12.79 ± 0.45	14.90 ± 0.75
	12.44–15.05	12.14–14.44	11.91–14.91	11.95–13.41	13.61–15.59
PL	16.66 ± 0.74	17.27 ± 0.95	17.08 ± 1.00	16.05 ± 0.92	18.46 ± 0.34
	15.02–18.26	15.46–19.28	15.23–19.43	15.07–17.96	18.02–18.96
IFL	5.59 ± 0.49	5.79 ± 0.59	5.37 ± 0.57	5.77 ± 0.67	6.19 ± 0.40
	4.35–6.53	4.34–6.65	3.39–6.30	4.72–6.87	5.67–6.57
WIF	2.52 ± 0.20	2.52 ± 0.20	2.45 ± 0.20	2.48 ± 0.26	2.78 ± 0.12
	2.03–2.92	2.23–2.95	2.13–2.93	2.20–2.99	2.57–2.89
GPB	6.72 ± 0.27	6.68 ± 0.35	6.56 ± 0.27	6.42 ± 0.25	7.11 ± 0.21
	6.13–7.22	6.12–7.85	5.83–7.19	6.01–6.80	6.84–7.32
LTB	5.29 ± 0.39	5.84 ± 0.52	5.54 ± 0.52	5.32 ± 0.52	5.02 ± 0.42
	4.10–5.95	4.99–7.32	4.40–6.70	4.66–6.06	4.61–5.81
ULMM	5.67 ± 0.24	5.76 ± 0.30	5.48 ± 0.26	5.33 ± 0.22	5.93 ± 0.16
	5.27–6.23	5.19–6.57	4.69–6.12	4.84–5.63	5.74–6.10
ULMD	8.83 ± 0.59	8.86 ± 0.68	8.77 ± 0.76	8.30 ± 0.81	9.89 ± 0.33
	7.56–10.58	7.23–10.19	7.36–10.57	7.58–9.86	9.49–10.27
ML	15.99 ± 0.69	16.70 ± 1.13	16.27 ± 1.12	15.28 ± 0.52	18.10 ± 0.62
	14.58–17.25	13.66–19.00	13.61–18.50	14.34–16.01	16.90–18.60
LLMM	5.69 ± 0.20	5.66 ± 0.33	5.44 ± 0.32	5.21 ± 0.21	5.87 ± 0.15
	5.28–6.09	4.85–6.34	4.95–6.44	4.81–5.40	5.69–6.10
LLMD	4.57 ± 0.46	4.61 ± 0.49	4.61 ± 0.58	4.28 ± 0.46	5.25 ± 0.31
	3.77–5.78	3.63–5.98	3.35–5.86	3.59–5.31	4.77–5.60

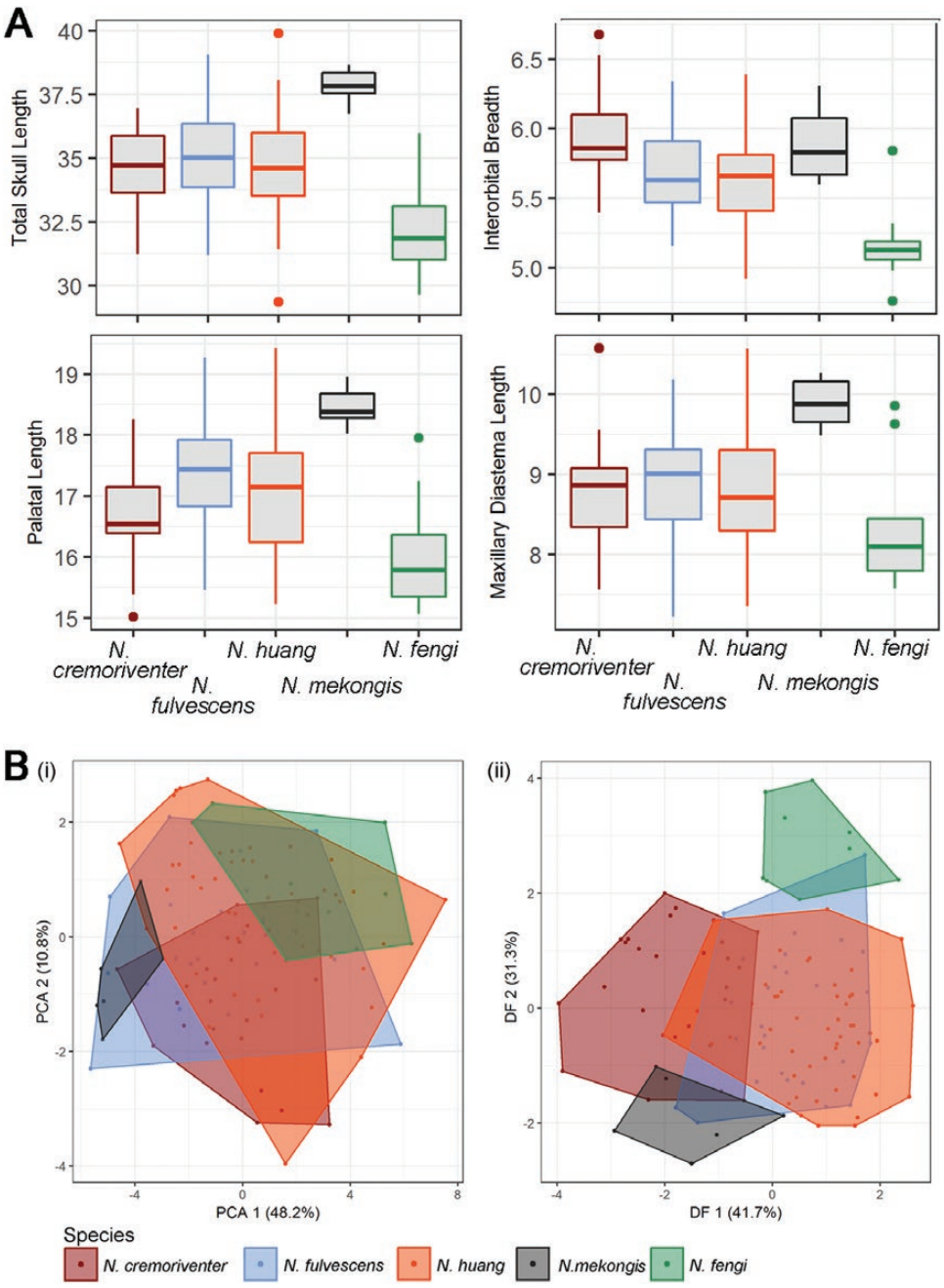

Figure 4. Morphological variation of CMs within the NFSC in China. A, boxplots of the main diagnostic craniodental measurements of the NFSC members in China obtained by comparing the TLC (total length of the cranium), SDO (shortest distance between orbits), PL (palatal length) and ULMD (length of the maxillary diastema) values between species. B, scatterplots of the principal components (i) and discriminant functions (ii) of the CMs of the NFSC.

m (200–2300 m) and an annual precipitation of ~1300 mm (784–1974 mm). *Niviventer fulvescens* inhabits south-western Yunnan Province to the south-eastern Himalayan Mountains, with an average elevation of 2065 m (1300–2900 m). *Niviventer* sp. 3 ranges from the south to the north of Indochina and inhabits a lower elevation than its congeners (416 m, 50–2300 m). *Niviventer* sp. 1 is known only from Jilong, Tibet, where the elevations of the sampling sites for this species range from 2900 to 3200 m. This species inhabits a higher elevation than other species within the NFSC. Sympatric species include *N. eha* (trapped from 2900 to 3200 m) and *N. fulvescens* (trapped approximately 2900 m).

Figure 5. Comparison of the skin and skull of *N. fengi* with closely related species. *Niviventer fengi*, A1, A2, IOZCAS JL17111; A3, A4, IOZCASJL17059, HBL = 146. *Niviventer fulvescens*, B1, B2, IOZCAS JD113; B3, B4, JL17057, HBL = 120. *Niviventer huang*, C1, C2, NHM 98.11.1.16; C3, C4, IOZCAS HN2017242, HBL = 125. *Niviventer mekongis*, D1, D2, NHM 26.11.17.13; D3, D4, ZIN102439, HBL = 134. *Niviventer cremoriventer*, E1, E2, KMIOZCAS; E3, E4. KMIOZCAS, HBL = 107.

The distribution of *N. huang* in Hainan implies a recent invasion by this species of Hainan Island via the Qiongzhou Strait. Hainan Island is only 20 km from the mainland at the narrowest point (Zhu, 2016). Dispersal of *N. huang* into Hainan likely occurred during the late Pleistocene, when the faunal exchange between mainland China and Hainan was made possible by a lower sea level and the formation of a land bridge across the Qiongzhou Strait (Huang *et al.*, 2013). However, the exchange of fauna and flora between Hainan and Vietnam involved more frequent events occurring earlier than the arrival of *N. huang*. For example, the Hainan flora shows high similarity to the flora of Vietnam at the family and generic levels (Zhu, 2016). Discovery of the Hainan gymnure, *Neohylomys hainanensis* Shaw & Wong, 1959, in northern Vietnam (previously considered a rare and poorly known endemic species of Hainan) also emphasize the connection of Hainan Island to northern Vietnam and Guangxi (Abramov *et al.*, 2018).

Taxonomic account of the NFSC in China

According to the results of the above analyses integrating molecular data, EMs and CMs to identify variation among NFSC genetic lineages in China, we provide a comprehensive taxonomic revision of the NFSC. Morphological comparisons and quantitative analyses revealed an underestimation of species diversity within the NFSC, with two additional species recognized. Overall, five species within the NFSC, namely, *N. cremoriventer*, *N. fengi*, *N. fulvescens*, *N. huang* and *N. mekongis* are found in China.

The biodiversity on the mainland Southeast Asian peninsula and surrounding islands has been well studied in a morphological context (Miller, 1913; Tate, 1936; Lekagul & McNeely, 1977; Musser, 1981; Pimsai *et al.*, 2014), but scarce molecular data, or a lack of morphological data for voucher specimens, hinder a better taxonomic delimitation and understanding of the phylogenetic placement of the species endemic to this region, leaving both the boundaries and

Table 3. Morphological differences between species within the NFSC as determined by LSD tests. Abbreviations are the same as in Table 2. CPCA, MANOVA results based on PCA scores; CLDA, MANOVA results based on LDA scores. Original data of EMS and CMs are provided in Supplementary Data S3 and S4. Species with fewer than three individual specimens were excluded from the analyses. *$P < 0.05$.

		NC	NF	NH	NFE
NC	BM	-------			
	HBL	-------			
	TL	-------			
	HFL	-------			
	EL	-------			
	CPCA	-------			
	CLDA	-------			
NF	BM	0.436	-------		
	HBL	0.749	-------		
	TL	0.069	-------		
	HFL	0.464	-------		
	EL	0.228	-------		
	CPCA	<0.001*	-------		
	CLDA	<0.001*	-------		
NH	BM	0.041*	0.036*	-------	
	HBL	0.041*	0.098	-------	
	TL	0.228	<0.001*	-------	
	HFL	0.017*	0.003*	-------	
	EL	0.483	0.293	-------	
	CPCA	<0.001*	<0.001*	-------	
	CLDA	<0.001*	<0.001*	-------	
NFE	BM	0.225	0.012*	<0.001*	-------
	HBL	0.566	0.169	0.018*	-------
	TL	<0.001*	<0.001*	<0.001*	-------
	HFL	0.006*	<0.001*	<0.001*	-------
	EL	0.665	0.410	0.840	-------
	CPCA	<0.001*	<0.001*	<0.001*	-------
	CLDA	<0.001*	<0.001*	<0.001*	-------
NM	BM	0.013*	0.014*	0.221	<0.001*
	HBL	0.192	0.018*	0.181	<0.002*
	TL	0.586	<0.001*	0.005*	<0.001*
	HFL	<0.001*	<0.001*	0.018*	<0.001*
	EL	0.459	0.559	0.842	0.758
	CPCA	<0.001*	<0.001*	<0.001*	<0.001*
	CLDA	<0.001*	<0.001*	<0.001*	<0.001*

overall range of the species unclear. For example, the species status of the fourth lineage (*N.* sp. 2), from Indonesia (west Java, Cibodas, Mt. Gede) and Laos (Khammouane, Nakai Plateau), recognized based on *Cytb*, could not be identified in the present study, because no detailed morphological information is available for these specimens.

We provide a comprehensive taxonomic revision of the NFSC in China, and all of our original data are available in GenBank or the original supplementary files in hope of promoting a more comprehensive study of these species across Asia.

ORDER RODENTIA

SUBORDER MYOMORPHA

SUPERFAMILY MUROIDEA

FAMILY MURIDAE

SUBFAMILY MURINAE

GENUS *NIVIVENTER* MARSHALL, 1976

NIVIVENTER CREMORIVENTER (MILLER, 1900)

(FIG. 5E1–E4)

Sundaic arboreal niviventer or dark-tailed tree rat.

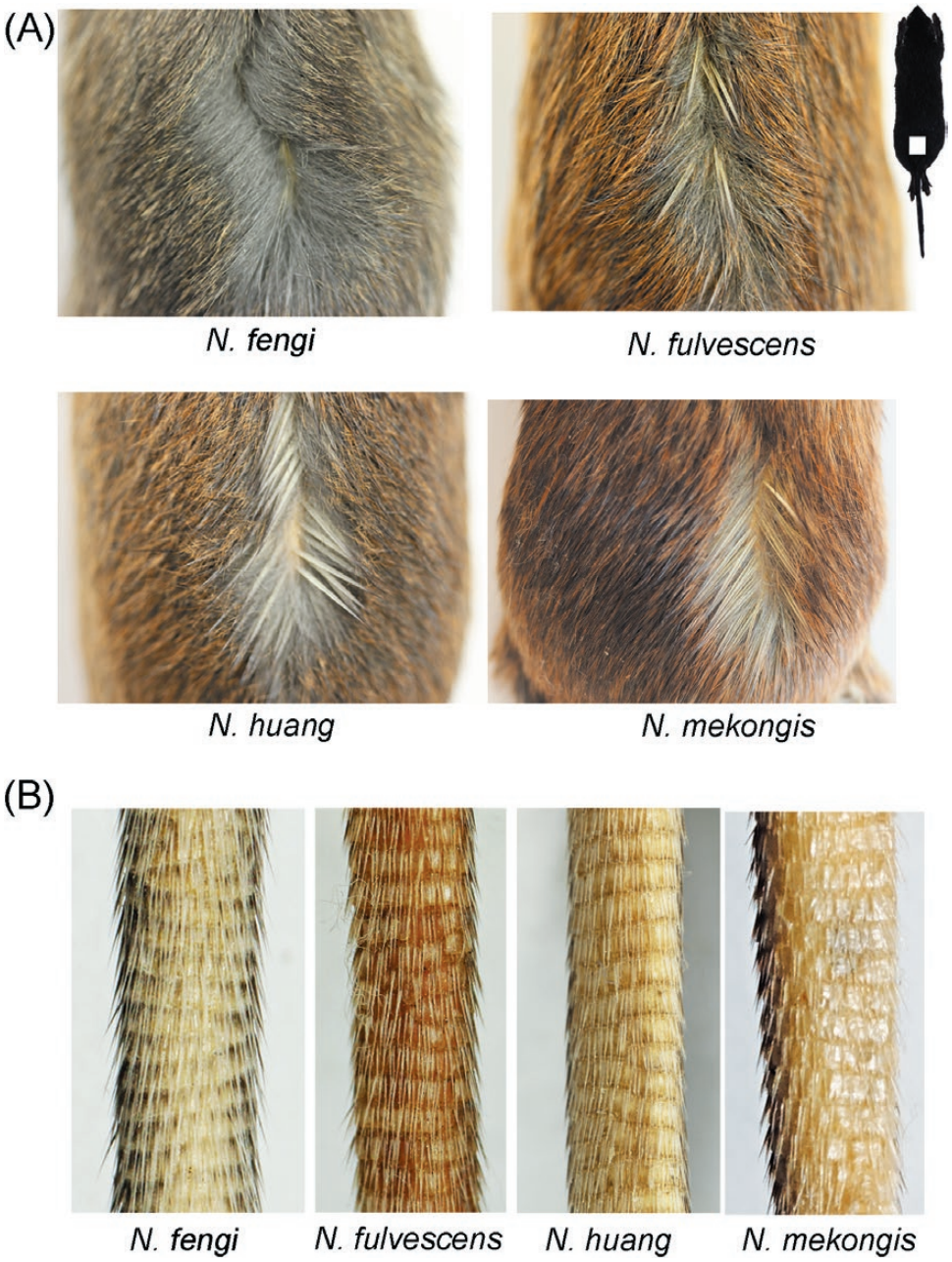

Figure 6. Diagnostic external traits for the differentiation of *N. fengi*, *N. huang*, *N. fulvescens* and *N. mekongis*. A, dorsal hairs. B, ventral tail. Note that *N. fengi* has a hairier tail and darker skin without spines.

Mus cremoriventer Miller, 1900a: 144. Southern peninsular Thailand, Trong, Trang Province, Thailand.

Mus flaviventer Miller, 1900b: 204. Puki Jimaja, Anambas Islands.

Mus gilbiventer Miller, 1903: 35. Sullivan Island, Mergui Archipelago, Burma.

Mus kina Bonhote, 1903: 124. Mount Kinabalu, Borneo.

Epimys barussanus Miller, 1911: 26. Mojeia River, Nias Island, Sumatra.

Epimys mengurus Miller, 1911: 27. Bukit Menguru, Billiton Island, Sumatra.

Epimys spatulatus Lyon, 1911: 111. Pulo Lamukotan, Borneo.

Epimys solus Miller, 1913: 22. Pulo Teratau Island, Malay Peninsula.

Rattus cremoriventer cretaceiventer Robinson & Kloss, 1919: 377. Tjibodas, Java.

Rattus cremoriventer malawali Chasen & Kloss, 1932: 32. Mallewalle Island, Borneo.

Rattus cremoriventer sumatrae Bartels, 1937: 123. Bandjarnegri, Wai Semangka, Lampoengs, Sumatra.

Holotype: USNM 86770, skin and skull of an adult male collected by W. L. Abbott on 16 January 1899. Mountain of Trong, Trang Province, Lower Siam (Thailand), at approximately 900 m, approximate coordinates: 7.433 N, 99.85 E.

Measurements (in mm): EMs and CMs of holotype provided by Miller (1900) are as follows: total length = 317, HBL = 146, TL = 171, pencil at the tip of the tail = 8, EL = 17, ear from crown = 13 and width of ear = 12. Greatest length of skull = 34, basal length = 28, basilar length = 25, palatal length = 13.4, least width of palate between anterior molars = 3.4, diastema = 8.2, length of incisive foramen = 5.6, combined breadth of incisive foramina = 2.6, length of nasals = 11.8, combined breadth of nasals = 4, zygomatic breadth = 15.4, interorbital breadth = 6, mastoid breadth = 12.8, breadth of braincase over roots of zygomata = 14.8, depth of braincase at front of basioccipital = 10, frontal–palatal depth at posterior extremity of nasals = 7, least depth of rostrum immediately behind incisors = 6, maxillary toothrow (alveoli) = 6, width of front upper molar = 1.6, mandible = 15.6 and mandibular toothrow (alveoli) = 6.

BM (g), EMs and CMs (mean ± 1 SD, range, mm) from museum specimens: BM = 62.1 ± 6.40 (51–68, $N = 10$). EMs of ten adult specimens: HBL = 133 ± 6.04, TL = 178.13 ± 14.80, HFL = 26.80 ± 0.92 and EL = 19.20 ± 1.03. CMs from 29 intact adult specimens: TLC = 34.67 ± 1.41, NL = 12.31 ± 0.59, GWS = 5.78 ± 0.58, SDO = 5.93 ± 0.25, ZB = 15.50 ± 0.93, GMB = 13.87 ± 0.68, PL = 16.66 ± 0.74, IFL = 5.59 ± 0.49, WIF = 2.52 ± 0.20, GPB = 6.72 ± 0.27, LTB = 5.29 ± 0.39, ULMM = 5.67 ± 0.24, ULMD = 8.83 ± 0.59, ML = 15.99 ± 0.69, LLMM = 5.69 ± 0.20 and LLMD = 4.57 ± 0.46. Original measurements are given in Supporting Information, Table S2.

Diagnosis: Niviventer cremoriventer is a medium-sized species with spines mixed with soft hairs on the dorsum. Dorsal coloration is overall bright orange or reddish brown and more yellowish on the sides. Feet have an overall brown colour and are covered with fine, short, white hairs. Tail is uniformly dark with a short tuft at the tip. Skull of *N. cremoriventer* is appreciably gracile, with undeveloped supraorbital ridges and the rostrum is narrow.

Distribution: This species occupies the widest distribution range of members of the NFSC and is widely distributed in the Malay Peninsula, Sunda Islands and Southeast Asia. It was also discovered in Modao River, Jingdong, Yunnan Province, China.

Comments: Musser (1973) presented a detailed description of the external and craniodental features of the species and discussed the taxonomic identity of *N. cremoriventer* in relation to similar taxa from Southeast Asia. Musser (1973, 1981) considered the Indochinese species *N. langbianis* (Robinson & Kloss, 1922) as the closest morphological and likely phylogenetic relative of *N. cremoriventer*, which is now assigned to a species in the genus *Chiromyscus* (Balakirev *et al.*, 2014; Jing *et al.*, 2007). However, these two species differ in the colour of the pelage and the size and proportions of external, cranial and dental features. The brownish grey upper parts with pale yellow and olive tones of *C. langbianis* are in striking contrast to the orange or reddish brown upper parts of *N. cremoriventer* (Musser 1973). Balakirev *et al.*, (2014) published figures of the holotype of *N. cremoriventer* (see fig. 6 in Balakirev *et al.*, 2014) and noted that the tail of this species was long, slender and hairy. These characteristics are different from those of other species within the NFSC.

The wide distribution of *N. cremoriventer* in Southeast Asia requires a more detailed study of the genetic diversity and morphological differentiation of this species, which might include cryptic species (Denys *et al.*, 2017). However, the present study included only data from GenBank, leaving a large area in Southeast Asia unsampled. Therefore, the intraspecific genetic differentiation of this species could not be clarified here.

Sympatric species: In China, *N. cremoriventer* has an overlapping distribution with *C. langbianis*, *N. bukit*, and *N. mekongis*. It is a typical rat of low and middle elevations (183–275 m) with a uniformly dark tail.

NIVIVENTER FULVESCENS (GRAY, 1847)

(FIGS 5B, 6)

Indomalayan niviventer, chestnut white-bellied rat.

Mus fulvescens Grey, 1847: 18. Nepal.
Mus caudatior Hodgson, 1849: 203. Nepal.

Holotype: NHM 45.1.8.376. Collected by B. H. Hodgson. The holotype is badly damaged. The animal

is small and immature, with the dorsal and ventral coat missing in several places.

Type locality: Nepal.

Measurements: No measurements were available for the holotype. BM, EMs and CMs (mean ± 1 SD, range, BM in g, measurements in mm) from molecular vouchers and museum specimens: BM = 66.82 ± 14.04 (40–91, *N* = 37). EMs of 37 adult specimens: HBL = 131.60 ± 11.18, TL = 187.74 ± 14.94, HFL = 27.22 ± 2.01 and EL = 20 ± 2.50. CMs from 29 intact adult specimens: TLC = 15.15 ± 1.73, NL = 12.92 ± 1.22, GWS = 5.40 ± 0.44, SDO = 5.65 ± 0.30, ZB = 15.09 ± 1.24, GMB = 13.28 ± 0.61, PL = 17.27 ± 0.95, IFL = 5.79 ± 0.59, WIF = 2.52 ± 0.20, GPB = 6.68 ± 0.35, LTB = 5.84 ± 0.52, ULMM = 5.76 ± 0.30, ULMD = 8.86 ± 0.68, ML = 16.70 ± 1.13, LLMM = 5.66 ± 0.33 and LLMD = 4.61 ± 0.49.

Diagnosis: Niviventer fulvescens can be distinguished from other species within the NFSC by its longer tail and ears. It could be easily mistaken for *N. huang*, but *N. fulvescens* inhabits higher elevations.

Distribution: Nepal, south-western China and northern Indochina. In China it is distributed in higher mountains from south-western Yunnan to south-eastern Tibet.

Comments: Niviventer fulvescens is taxonomically the most ambiguous species of the NFSC. Previous studies largely overestimated the distribution range of this species (Allen, 1938; Musser & Carleton, 2005). According to molecular voucher specimens, it inhabits middle- to high-elevation mountains in south-western Yunnan and south-eastern Tibet. The present analyses identifies two major genetic lineages within *N. fulvescens* (Fig. 1); the first lineage was confined to south-eastern Tibet along the Himalayan Mountains. The second lineage was distributed in south-western Yunnan, western Sichuan and northern Vietnam. Pelage coloration differs slightly between these two genetic lineages. The lineage from south-eastern Tibet has a darker coloration than those from Yunnan. Spines are more prominent in individuals from Yunnan than in those from the other locations.

Sympatric species: The distribution of *N. fulvescens* largely overlaps with those of *N. andersoni* and *N. niviventer*. The last two species also inhabit middle- to high-elevation mountains in southern China. *Niviventer andersoni* is distinguishable by its larger size and bicoloured tail (the one-third near the tip is white) and *N. niviventer* belongs to the NNSC and has a darker pelage.

NIVIVENTER HUANG (BONHOTE, 1905)

(FIGS 5C, 6)

Lowland niviventer, Lowland white-bellied rat.

Mus huang Bonhote, 1905: 19. Kuatun (Guadun), north-western Fokien (Fujian Province), China.

Mus ling Bonhote, 1905: 19. Ching Fen Ling (Qingfeng Ling), north-western Fokien (Fujian Province), China.

Rattus huang vulpicolor Allen, 1926: 14. Namting River, Yunnan, China.

Rattus flavipilis Shih, 1930: 2. Luoxiang, Guangxi, China.

Rattus flavipilis minor Shih, 1930: 7. Kutchen, Loshiang, Kwangsi (Guangxi Province), China.

Rattus wongi Shih, 1931: 6. Yaoshan, Kwantung (Guangdong Province), China.

Holotype: NHM 98.11.1.16, skin and skull of an adult male collected by J. D. La Touche on 24 April 1898. Kuatun (Guadun), north-western Fokien (Fujian Province), China.

Measurements: EMs and CMs of the holotype (Bonhote, 1905) are as follows: HBL = 155, TL = 188, HF = 30 and EL = 16; greatest length of skull = 37, basilar length = 27 and PL = 17; diastema = 9.5; incisive foramina = 7; length of nasals = 14; interorbital breadth = 6; greatest breadth of braincase = 14; and length of molar series (alveoli) = 6.

BM, EMs and CMs (mean ± 1 SD, range) of molecular vouchers and museum specimens: BM = 73.67 ± 17.81 (40.00–120.40, *N* = 105). EMs of 105 adult specimens: HBL = 135.36 ± 12.30, TL = 172.08 ± 11.84, HFL = 28.11 ± 1.53 and EL = 19.64 ± 1.81. CMs from 50 intact adult specimens: TLC = 34.78 ± 2.01, NL = 12.85 ± 1.27, GWS = 5.32 ± 0.41, SDO = 5.65 ± 0.32, ZB = 14.89 ± 1.19, GMB = 13.13 ± 0.60, PL = 17.08 ± 1.00, IFL = 5.37 ± 0.57, WIF = 2.45 ± 0.20, GPB = 6.56 ± 0.27, LTB = 5.54 ± 0.52, ULMM = 5.48 ± 0.26, ULMD = 8.77 ± 0.76, ML = 16.27 ± 1.12, LLMM = 5.44 ± 0.32 and LLMD = 4.61 ± 0.58.

Diagnosis: Niviventer huang has a bright yellowish brown colour on the dorsum and is more fulvous on the sides. Spines are thick and whitish and abundant on the rump. Feet are generally whitish, with a golden patch on the dorsal surface of the metatarsus. Tail is clearly bicoloured, dark brown in dorsal view, white in ventral view, and covered with short whitish hairs not covering the scales.

Distribution: This species is distributed in central and eastern China, including Sichuan, Yunnan, Guangxi, Guangdong, Fujian, Zhejiang, Hunan, Hubei, Guizhou and Hainan Island.

Comments: Based on molecular data, three genetic lineages were present in *N. huang*: the first lineage includes individuals from Yunnan and Fujian Provinces, the second lineage includes samples from Hainan Province and the third lineage includes individuals from Sichuan, Chongqing, Hunan, Hubei, Guangdong and Guangxi Provinces (Figs 1, 2). In line with this result, Bonhote (1905) stated that the type of *N. huang* (from Fujian Province) is indistinguishable from a specimen collected in Ngau-tchi-lea Mountain (now Five-Finger Mountain) in Hainan Province.

Moreover, Bonhote (1905) described *N. ling* from the same province (Fujian). Notably, Bonhote mentioned that *N. ling* also occurs in Kuatun (type locality of *N. huang*) and that both taxa closely resemble each other. Based on our direct examination of the holotypes of *N. huang* and *N. ling*, we found the differences between these species subtle, mainly related to slight differences in fur colour and body size (Supporting Information, Fig. S4; Table S3). Therefore, given the subtle differences between the types, that both taxa occur in the same locality (Kuatun, according to Bonhote) and all sequences of Fujian provinces cluster together, we treat *N. ling* as junior synonym of *N. huang*.

Sympatric species: *Niviventer huang* occurs in sympatry with *N. mekongis* in south China, and the confirmed overlapping records are from Lincang Snow Mountain, Lincang and Menghai, both in southern Yunnan Province.

NIVIVENTER MEKONGIS (ROBINSON & KLOSS, 1922) **COMB. NOV.**

(FIGS 5D, 6D)

Mekong niviventer, Mekong white-bellied rat.

Rattus blythi mekongis Robinson & Kloss, 1922: 96. Bak Mat on the Mekong River (N 18° 53′), Laos.
Rattus bukit condorensis Kloss, 1926: 357. Pulo Condore, near the south-eastern coast of Cochinchina (Con Son Island, south Vietnam).

Holotype: NHM 7172/H (26.11.16.13), adult male collected by H. C. Robinson and C. Boden Kloss on 20 January 1920. Bak Mat on the Mekong River, Laos.

Measurements: EMs for holotype: HBL = 136, TL = 208, HFL = 29 and EL = 22. Robinson and Kloss (1922) provided the following CMs (in mm) for the holotype: greatest length of skull = 39.4, condylobasilar length = 33.0, diastema = 10.3, upper molar row = 6.5, length of palatal foramina = 7.0, length of nasals = 15.0, combined nasal breadth = 4.0 and zygomatic breadth = 17.9.

BM (g), EMs and CMs (mean ± 1 SD, range) of molecular vouchers and museum specimens: BM = 78.98 ± 22.49 (46.40–126.00, *N* = 18). EMs of 18 adult specimens: HBL = 139.08 ± 15.37, TL = 181.18 ± 16.60, HFL = 28.98 ± 1.62 and EL = 19.72 ± 1.31. CMs from six intact adult specimens: TLC = 37.84 ± 0.70, NL = 14.53 ± 1.22, GWS = 5.64 ± 0.33, SDO = 5.89 ± 0.29, ZB = 16.92 ± 0.63, GMB = 14.90 ± 0.75, PL = 18.46 ± 0.34, IFL = 6.19 ± 0.40, WIF = 2.78 ± 0.12, GPB = 7.11 ± 0.21, LTB = 5.02 ± 0.42, ULMM = 5.93 ± 0.16, ULMD = 9.89 ± 0.33, ML = 18.10 ± 0.62, LLMM = 5.87 ± 0.15 and LLMD = 5.25 ± 0.31.

Diagnosis: *Niviventer mekongis* has a markedly reddish brown colour on the dorsum, which is similar to the coloration of *N. lepturus* and *N. fraternus*. However, *N. fraternus* has a clear ochraceous-tawny patch on the chest and a longer tail (TL = 231) than *N. mekongis*, and the hairs of *N. lepturus* is soft and woolly (Jentink 1880). The TL and HFL of *N. mekongis* are clearly longer than those of *N. huang* (Fig. 4; Tables 2, 3). PCA and LDA of craniodental measurements reveals significant difference between this species and other species (Table 3).

Distribution: *Niviventer mekongis* is confined to Vietnam, Laos and southern Yunnan and Guangxi Provinces of China.

Comments: Individuals of this species were assigned to *N. huang* by Balakirev *et al.*, (2011) and in subsequent studies (Lu *et al.*, 2015). However, both genetic distances (Table 1) and morphological differentiation (Table 3) support this lineage as an independent species. Among all formally described *Niviventer* taxa from South Asia, a large number of species or subspecies that resemble *N. fulvescens* have been established (see: Ellerman, 1940; Musser, 1973, 1981). Most of them were established based on specimens collected from southern Myanmar and southern Thailand, including *N. gracilis* from the Summit of Mount Mooleyit, northern Tenasserim, Myanmar, *N. lepidus* from Bok Pyin, southern Tenasserim, Myanmar, *N. pan* (Robinson & Kloss, 1914) from Ko Samui Island, Thailand and *N. blythi* from Shwegyin, Tenasserim, Myanmar. However, all of these taxa were described outside of the area where lineage *N.* sp. 3 was found. *Rattus blythi mekongis* Robinson & Kloss, 1922, from Bak Mat, Mekong River, Laos (N 18° 53′), seems to be the earliest available name for lineage *N.*

sp. 3 sampled from Laos, Vietnam and south-eastern Yunnan and Guangxi in China. the morphological characteristics of the specimens from this genetic lineage are in full agreement with the characteristics of holotype NHM 7172/H (26.11.16.13) (see Supporting Information, Fig. S4). *Rattus bukit condorensis* (Kloss, 1926) from Con Son Island, southern Vietnam, appears to be a synonym of this species. The specimens from Con Son Island were genetically closely related (based on *COI* gene sequences) to the mainland populations of *N. mekongis* (see Balakirev *et al.*, 2011).

Sympatric species: *Niviventer mekongis* occurs sympatrically with *N. cremoriventer* and *N. bukit*. *Niviventer cremoriventer* is easily distinguishable from *N. mekongis* by its uniformly black tail. *Niviventer bukit* is distinguishable from *N. mekongis* by its shorter TL and darker pelage colouration.

NIVIVENTER FENGI GE, FEIJÓ AND YANG SP. NOV.

(FIGS 5A, 6)

Jilong soft-furred niviventer, Tibetan white-bellied rat. lsid: zoobank.org:pub:A0C63287-87B3-42E0-BC0E-CACDE62A8137

Holotype: IOZCASJL17111, an adult male preserved as dry skin, skull and frozen tissue deposited at the Institute of Zoology, Chinese Academy of Sciences, Beijing. The holotype was collected by Drs Zhixin Wen and Yuanbao Du on 16 October 2017. The *Cytb*, *COI*, D-loop and *Rbp3* sequences of the holotype are archived in GenBank with accession numbers MN814475–MN814491, MN814581–MN814584, MN814634–MN814637 and MN814696–MN814698, respectively. EMs are as follows: BM = 47 g, HBL = 122, TL = 145, HFL = 25 and EL = 21. CMs are as follows: TLC = 31.72, NL = 10.44, GWS = 5.49, SDO = 5.14, ZB = 14.4, GMB = 12.79, PL = 15.34, IFL = 5.36, WIF = 2.23, GPB = 6.39, LTB = 4.66, ULMM = 5.25, ULMD = 7.8, ML = 15.46, LLMM = 5.25 and LLMD = 4.23.

BM, EMs and CMs of molecular vouchers and museum specimens: BM = 53.67 ± 14.03 (41–80, N = 15). EMs of 15 adult specimens: HBL = 126.47 ± 14.03, TL = 146.07 ± 14.19, HFL = 24.93 ± 1.49 and EL = 19.53 ± 1.46. CMs from nine intact adult specimens: TLC = 32.44 ± 1.98, NL = 11.49 ± 1.24, GWS = 5.36 ± 0.49, SDO = 5.17 ± 0.28, ZB = 14.84 ± 0.60, GMB = 12.79 ± 0.45, PL = 16.05 ± 0.92, IFL = 5.77 ± 0.67, WIF = 2.48 ± 0.26, GPB = 6.42 ± 0.25, LTB = 5.32 ± 0.52, ULMM = 5.33 ± 0.22, ULMD = 8.30 ± 0.81, ML = 15.28 ± 0.52, LLMM = 5.21 ± 0.21 and LLMD = 4.28 ± 0.46.

Type locality: Jilong Valley, Jilong County, Shigatse, Tibet, China (N 28.48493, E 85.22434; 3295 m). This region is characterized by alpine coniferous forest dominated by cypresses and an understorey of *Cremanthodium* sp., *Himalaiella nivea* (DC.) Raab-Straube (both Asteraceae) and *Rhodiola rosea* L. (Crassulaceae).

Paratype: IOZCASJL17059 (Fig. 5A3–4), an adult male preserved as dry skin, skull and frozen tissue collected on 15 October 2017 at 2900 m in Jilong Valley, Tibet, China (N 28.48099, E 85.22477; 2900 m). BM = 78 g, HBL = 146, TL = 180, HFL = 26, and EL = 20. CMs are as follows: TLC = 34.68, NL = 13.82, GWS = 5.77, SDO = 5.08, ZB = 15.97, GMB = 13.16, PL = 17.25, IFL = 6.87, WIF = 2.99, GPB = 6.57, LTB = 5.91, ULMM = 5.49, ULMD = 9.63, ML = 16.01, LLMM = 5.27 and LLMD = 4.44.

Additional specimens: Skins of IOZCASJL17051, IOZCASJL17201 and IOZCASJL17210 collected together with the type specimens. Skulls of IOZCASJL17062, IOZCASJL17071, IOZCASJL17075, IOZCASJL17079, IOZCASJL17107, IOZCASJL17201 and IOZCASJL17210 are intact and preserved with the skin specimens.

Sequenced molecular voucher specimens: Fifteen males, including IOZCASJL17051, IOZCASJL17059, IOZCASJL17062, IOZCASJL17063, IOZCASJL17070, IOZCASJL17071, IOZCASJL17075, IOZCASJL17076, IOZCASJL17078, IOZCASJL17079, IOZCASJL17082, IOZCASJL17202, IOZCASJL17111 and IOZCASJL17201; one female, IOZCASJL17107; and one specimen of unknown sex (badly damaged), IOZCASJL17100, which was collected at the same locality as the holotype and paratypes by Drs Zhixin Wen and Yuanbao Du.

Description: Smallest species in the NFSC, with dense and soft fur and without spines. HBL ranges from 110 to 140 mm and TL from approximately 118% to 127% of the HBL. Dorsal coloration brownish and finely sprinkled with yellowish. Individual dorsal hairs are mostly dark grey with yellowish tips. Guard hairs long and scattered on the dorsum, mainly in the posterior region; some show a bicolour pattern: black in the posterior half and white in the anterior half. Ventral colour uniformly white, contrasting sharply with the upper parts. Ears short, black and without evident hairs. Mystacial vibrissae long, with some extending beyond the posterior margin of the ear, black in the basal portion and paler distally. Forefeet covered with short, whitish hairs. Feet with a marked grey brownish patch in the medial portion of the metatarsal region, and the digits with whitish hairs. Tail hairy, with hairs spanning up to two scales, and at its tip forming a short, usually black tuft of approximately 15 mm. Tail

bicoloured, with the upper part darker and covered by black hairs and the venter part pale and covered by white hairs. Tail scales arranged in an annular pattern approximately 0.8 mm in length. Skull with a relatively short rostrum and rounded braincase. Its general dorsal profile nearly flat, particularly in the frontal region, where there is a shallow medial depression. Dorsolateral margins of the interorbital well defined by supraorbital ridges that extend to the lateral braincase. Zygomatic arches slightly expanded laterally, with their maxillary root lying anterior to the tooth row. Incisive foramina narrow and extending to the anterior margin of the tooth row. Intraparietal wide and short in the anterior-posterior plane. Palatal short and extending slightly beyond the posterior margin of the third molar. Auditory bullae small.

Diagnosis: Niviventer fengi is easily distinguished from all other species of the NFSC by its overall darker colour, the absence of spines, a brownish patch in the metatarsal region of the hindfoot and its hairier tail (Fig. 6A1, A2). All other species of the NFSC have a generally bright ochraceous or reddish brown colour and spines on the dorsum (Fig. 6A1; Musser, 1973, 1981). *Niviventer fengi* is also differentiated from its conspecifics by its smaller size, especially the proportionally smaller size of the tail, hindfoot, total length of the skull, length of maxillary diastema, interorbital breadth, PL and ML (see Tables 2, 3; Fig. 4).

Distribution: This species is known from Jilong Valley, Rikaze, Tibet Province, China, near the Nepalese border.

Etymology: We named this new species in honour of Prof. Zuojian Feng from IOZCAS for the great contribution to the study of mammals in China.

Comments: The general morphology of *N. fengi* is similar to that of *N. excelsior*, including its soft fur, but this species is significantly smaller than *N. excelsior* (BM = 67 ± 13.64, HBL = 133.14 ± 9.788, TL = 205.57 ± 12.98, HFL = 30.71 ± 2.05 and EL = 22.71 ± 0.95), which is endemic to the south-western mountainous area of China (Ge *et al.*, 2017).

Sympatric species: Niviventer fengi is sympatric with *N. fulvescens* and *N. eha*, but they are distinct in external morphology.

ACKNOWLEDGEMENTS

We greatly appreciate Prof. Alfried P. Vogler from the NHM for his help during the early academic stage of Deyan Ge. We thank Roberto Portela Miguez, Paula Jenkins and Louise Tomsett from NHM (London, UK), Song Li from KMIOZCAS (Kunming, China), Xichao Zhu and Yang Yang from IOZCAS (Beijing, China), Yuchun Li from MCSU (Weihai, China), Bruce D. Patterson from FMNH (Chicago, USA), Eugenia R. Maksimova and Olga V. Makarova from ZIN (Saint Petersburg, Russia) for their assistance with the specimens preserved under their supervision. Yuanbao Du assisted with field work. We also thank Profs Mohd Tajuddin Abdullah and Jacob A. Esselstyn for sharing important literature. We appreciate the help of associate editor Prof. Gregory Adler for his help and encouragement on publication of this manuscript. Deyan Ge is sponsored by the Newton Advanced Fellowship of the Royal Society, United Kingdom (NA150142) and a grant from the National Nature Science Fund of China (31872958). This research is also sponsored by the National Special Fund on Basic Research of Science and Technology in China (2014FY110100, 2014FY210200) and by a grant from the Key Laboratory of Zoological Systematics and Evolution of the Chinese Academy of Sciences (Y229YX5105). Alexei V. Abramov is sponsored by the International Fellowship for Distinguished Scientists, Chinese Academy of Sciences (Ref. 2017VBA0027) and in part by grants-in-aid from the Ministry of Science and Higher Education of Russian Federation, and the Ministry of Science and Higher Education of Russia (project AAAA-A19-119082990107-3). Anderson Feijó is financially supported by the Chinese Academy of Sciences President's International Fellowship Initiative (2018PB0040) and received a Visiting Scholarship from the Field Museum of Natural History, Chicago, USA.

REFERENCES

Abramov AV, **Meschersky IG**, **Rozhnov VV. 2009.** On the taxonomic status of the harvest mouse *Micromys minutus* (Rodentia: Muridae) from Vietnam. *Zootaxa* **2199:** 58–68.

Abramov AV, **Bannikova AA**, **Lebedev VS**, **Rozhnov VV. 2018.** A broadly distributed species instead of an insular endemic? A new find of the poorly known Hainan gymnure (Mammalia, Lipotyphla). *ZooKeys* **795:** 77–81.

Achmadi AS, **Esselstyn JA**, **Rowe KC**, **Maryanto I**, **Abdullah MT. 2013.** Phylogeny, diversity, and biogeography of Southeast Asian spiny rats (*Maxomys*). *Journal of Mammalogy* **94:** 1412–1423.

Allen GM. 1938. *The mammals of China and Mongolia*. New York: American Museum of Natural History.

Aplin KP, **Suzuki H**, **Chinen AA**, **Chesser RT**, **Ten Have J**, **Donnellan SC**, **Austin J**, **Frost A**, **Gonzalez JP**, **Herbreteau V**, **Catzeflis F**, **Soubrier J**, **Fang YP**, **Robins J**, **Matisoo-Smith E**, **Bastos ADS**, **Maryanto I**,

Sinaga MH, **Denys C**, **Van den Bussche RA**, **Conroy C**, **Rowe K**, **Cooper A. 2011.** Multiple geographic origins of commensalism and complex dispersal history of black rats. *PLoS One* **6:** e26357.

Balakirev AE, **Abramov AV**, **Rozhnov VV. 2011.** Taxonomic revision of *Niviventer* (Rodentia, Muridae) from Vietnam: a morphological and molecular approach. *Russian Journal of Theriology* **10:** 1–26.

Balakirev AE, **Abramov AV**, **Rozhnov VV. 2014.** Phylogenetic relationships in the *Niviventer-Chiromyscus* complex (Rodentia, Muridae) inferred from molecular data, with description of a new species. *ZooKeys* **451:** 109–136.

Bonhote JL. 1905. The mammalian fauna of China. Part I. Murinae. *Proceedings of the Zoological Society of London* **1905:** 384–397.

Brunke J, **Radespiel U**, **Russo IR**, **Bruford MW**, **Goossens B. 2019.** Messing about on the river: the role of geographic barriers in shaping the genetic structure of Bornean small mammals in a fragmented landscape. *Conservation Genetics* **20:** 691–704.

Delhey K. 2019. A review of Gloger's rule, an ecogeographical rule of colour: definitions, interpretations and evidence. *Biological Reviews* **94:** 1294–1316.

Denys C, **Taylor PJ**, **Burgin CJ**, **Aplin KP**, **Fabre PH**, **Haslauer R**, **Woinarski JC**, **Breed WG**, **Menzies JL. 2017.** Family Muridae. In: Wilson DE, Lacher TE, Mittermeier RA, eds. *Handbook of the mammals of the world*, **Vol. 7, rodents II**. Barcelona: Lynx Edicions.

Edgar RC. 2004. MUSCLE: multiple sequence alignment with high accuracy and high throughput. *Nucleic Acids Research* **32:** 1792–1797.

Ellerman JR. 1940. The families and genera of living rodents. 1. With a list of named forms (1758–1936). In: Hayman RW, Holt GWC, eds. *Rodents other than Muridae*, **Vol. 1**. London: British Museum.

Fujisawa T, **Barraclough TG. 2013.** Delimiting species using single-locus data and the generalized mixed yule coalescent approach: a revised method and evaluation on simulated data sets. *Systematic Biology* **62:** 707–724.

Ge DY, **Lu L**, **Cheng JL**, **Xia L**, **Chang YB**, **Wen ZX**, **Lv X**, **Du YB**, **Liu QY**, **Yang QS. 2017.** An endemic rat species complex is evidence of moderate environmental changes in the terrestrial biodiversity centre of China through the late Quaternary. *Scientific Reports* **7:** 46127.

Ge DY, **Lu L**, **Xia L**, **Du YB**, **Wen ZX**, **Cheng JL**, **Abramov AV**, **Yang QS. 2018.** Molecular phylogeny, morphological diversity, and systematic revision of a species complex of common wild rat species in China (Rodentia, Murinae). *Journal of Mammalogy* **99:** 1350–1374.

Ge DY, **Lu L**, **Abramov AV**, **Wen ZX**, **Cheng JL**, **Xia L**, **Vogler AP**, **Yang QS. 2019.** Coalescence models reveal the rise of the white-bellied rat (*Niviventer confucianus*) following the loss of Asian megafauna. *Journal of Mammalian Evolution* **26:** 423–434.

Goncalves GL, **Maestri R**, **Moreira GRP**, **Jacobi MAM**, **Freitas TRO**, **Hoekstra HE. 2018.** Divergent genetic mechanism leads to spiny hair in rodents. *PLoS One* **13:** e0202219.

Gorog AJ, **Sinaga MH**, **Engstrom MD. 2004.** Vicariance or dispersal? Historical biogeography of three Sunda shelf murine rodents (*Maxomys surifer*, *Leopoldamys sabanus* and *Maxomys whiteheadi*). *Biological Journal of the Linnean Society* **81:** 91–109.

Hammer O, **Harper DAT**, **Ryan PD. 2001.** PAST: paleontological statistics software package for education and data analysis. *Palaeontologia Electronica* **4:** 9.

He K, **Jiang XL. 2015.** Mitochondrial phylogeny reveals cryptic genetic diversity in the genus *Niviventer* (Rodentia, Muroidea). *Mitochondrial DNA* **26:** 48–55.

Huang Y, **Guo X**, **Ho SY**, **Shi H**, **Li J**, **Li J**, **Cai B**, **Wang Y. 2013.** Diversification and demography of the oriental garden lizard (*Calotes versicolor*) on Hainan Island and the adjacent mainland. *PLoS One* **8:** e64754.

Jansa SA, **Barker FK**, **Heaney LR. 2006.** The pattern and timing of diversification of Philippine endemic rodents: evidence from mitochondrial and nuclear gene sequences. *Systematic Biology* **55:** 73–88.

Jentink FA. 1880. On some hitherto undescribed species of *Mus* in the Leyden Museum. *Notes from the Leyden Museum* **2:** 13–19.

Jing MD, **Yu HT**, **Wu SH**, **Wang W**, **Zheng XG. 2007.** Phylogenetic relationships in genus *Niviventer* (Rodentia: Muridae) in China inferred from complete mitochondrial cytochrome *b* gene. *Molecular Phylogenetics and Evolution* **44:** 521–529.

Kapli P, **Lutteropp S**, **Zhang J**, **Kobert K**, **Pavlidis P**, **Stamatakis A**, **Flouri T. 2017.** Multi-rate Poisson tree processes for single-locus species delimitation under maximum likelihood and Markov chain Monte Carlo. *Bioinformatics* **33:** 1630–1638.

Kumar S, **Stecher G**, **Li M**, **Knyaz C**, **Tamura K. 2018.** MEGA X: molecular evolutionary genetics analysis across computing platforms. *Molecular Biology and Evolution* **35:** 1547–1549.

Lanfear R, **Frandsen PB**, **Wright AM**, **Senfeld T**, **Calcott B. 2017.** PartitionFinder 2: new methods for selecting partitioned models of evolution for molecular and morphological phylogenetic analyses. *Molecular Biology and Evolution* **3:** 772–773.

Latinne A, **Waengsothorn S**, **Rojanadilok P**, **Eiamampai K**, **Sribuarod K**, **Michaux JR. 2013.** Diversity and endemism of Murinae rodents in Thai limestone karsts. *Systematics and Biodiversity* **11:** 323–344.

Lekagul B, **McNeely JA. 1977.** *Mammals of Thailand*. Bangkok: Association for the Conservation of Wildlife, Thailand.

Lu L, **Ge DY**, **Chesters D**, **Ho SYW**, **Ma Y**, **Li GC**, **Wen ZX**, **Wu YJ**, **Wang J**, **Xia L**, **Liu JL**, **Guo TY**, **Zhang XL**, **Zhu CD**, **Yang QS**, **Liu QY. 2015.** Molecular phylogeny and the underestimated species diversity of the endemic white-bellied rat (Rodentia: Muridae: *Niviventer*) in Southeast Asia and China. *Zoologica Scripta* **44:** 475–494.

Luo AR, **Ling C**, **Ho SYW**, **Zhu CD. 2018.** Comparison of methods for molecular species delimitation across a range of speciation scenarios. *Systematic Biology* **67:** 830–846.

Martin T, **Marugan-Lobon J**, **Vullo R**, **Martin-Abad H**, **Luo ZX**, **Buscalioni AD. 2015.** A Cretaceous eutriconodont and integument evolution in early mammals. *Nature* **526:** 380–384.

Miller GS. 1900. Seven new rats collected by Dr W. L. Abbott in Siam. *Proceedings of the Biological Society of Washington* **13:** 137–150.

Miller GS. 1913. Fifty-one new Malayan mammals. *Smithsonian Institution Miscellaneous Collection* **61:** 1–30.

Mohd Salleh F, **Ramos-Madrigal J**, **Penaloza F**, **Liu S**, **Mikkel-Holger SS**, **Riddhi PP**, **Martins R**, **Lenz D**, **Fickel J**, **Roos C**, **Shamsir MS**, **Azman MS**, **Burton KL**, **Stephen JR**, **Wilting A**,**Gilbert MTP. 2017.** An expanded mammal mitogenome dataset from Southeast Asia. *Gigascience* **6:** 1–8.

Musser GG, **Carleton MD. 2005.** Superfamily Muroidea. In: Wilson DE, Reeder DM, eds. *Mammal species of the world, a taxonomic and geographic reference*. Baltimore: Johns Hopkins University Press.

Musser GG. 1973. Species-limits of *Rattus cremoriventer* and *Rattus langbianis*, murid rodents of Southeast Asia and the Greater Sunda Islands. *American Museum Novitates* **2525:** 1–65.

Musser GG. 1981. Results of the Archbold Expeditions. No. 105. Notes on systematics of Indo-Malayan murid rodents, and descriptions of a new genera and species from Ceylon, Sulawesi, and the Philippines. *Bulletin of the American Museum of Natural History* **168:** 229–334.

Nguyen LT, **Schmidt HA**, **von Haeseler A**, **Minh BQ. 2015.** IQ-TREE: a fast and effective stochastic algorithm for estimating maximum-likelihood phylogenies. *Molecular Biology Evolution* **32:** 268–274.

Osgood WH. 1932. Mammals of the Kelley-Roosevelts and Delacour Asiatic expeditions. *Field Museum of Natural History* **18:** 193–339.

Pahl T, **McLennan HJ**, **Wang Y**, **Achmadi AS**, **Rowe KC**, **Aplin K**, **Breed WG. 2018.** Sperm morphology of the Rattini – are the interspecific differences due to variation in intensity of intermale sperm competition? *Reproduction, Fertility and Development* **30:** 1434–1442.

Pimsai U, **Pearch MJ**, **Satasook C**, **Bumrungsri S**, **Bates PJJ. 2014.** Murine rodents (Rodentia: Murinae) of the Myanmar-Thai-Malaysian peninsula and Singapore: taxonomy, distribution, ecology, conservation status, and illustrated identification keys. *Bonn Zoological Bulletin* **63:** 15–114.

R Development Core Team. **2017.** *R: a language and environment for statistical computing*. Vienna: R Foundation for Statistical Computing.

Rambaut A, **Drummond AJ. 2007.** *Tracer v.1.5*. Available at: http://beast.bio.ed.ac.uk/Tracer (date last accessed, 20 November 2011).

Rensch B. 1929. *Das Prinzip geographischer Rassenkreise und das Problem der Artbildung*. Berlin: Gebrueder Borntraeger.

Robinson HC, **Kloss CB. 1922.** New mammals from French Indo-China and Siam. *Annals and Magazine of Natural History* **9:** 87–99.

Ronquist F, **Teslenko M**, **Van der Mark P**, **Ayres DL**, **Darling A**, **Hohna S**, **Larget B**, **Liu L**, **Suchard MA**, **Huelsenbeck JP. 2012.** MrBayes 3.2: efficient Bayesian phylogenetic inference and model choice across a large model space. *Systematic Biology* **61:** 539–542.

Smith AT, **Xie Y. 2008.** *A guide to the mammals of China*. Princeton and Oxford: Princeton University Press.

Stefen C, **Rudolf M. 2007.** Contribution to the taxonomic status of the Chinese rats *Niviventer confucianus* and *N. fulvescens*. *Mammalian Biology* **72:** 213–223.

Tate GHH. 1936. Some Muridae of the Indo-Australian region. *Bulletin of the American Museum of Natural History* **72:** 1–232.

Xia X. 2013. DAMBE5: a comprehensive software package for data analysis in molecular biology and evolution. *Molecular Biology and Evolution* **30:** 1720–1728.

Zhang J, **Kapli P**, **Pavlidis P**, **Stamatakis A. 2013.** A general species delimitation method with applications to phylogenetic placements. *Bioinformatics* **29:** 2869–2876.

Zhang B, **He K**, **Wan T**, **Chen P**, **Sun G**, **Liu SY**, **Nguyen TS**, **Lin L**, **Jiang XL. 2016.** Multi-locus phylogeny using topotype specimens sheds light on the systematics of *Niviventer* (Rodentia, Muridae) in China. *BMC Evolutionary Biology* **16:** 261.

Zhu H. 2016. Biogeographical evidences help revealing the origin of Hainan Island. *PLoS One* **11:** e0151941.

SUPPORTING INFORMATION

Additional Supporting Information may be found in the online version of this article at the publisher's web-site:

Table S1. Samples used in molecular analyses, the GenBank accession numbers of DNA fragments.
Table S2. EMs of specimens used in the present study.
Table S3. CMs of specimens used in the present study.
Table S4. Loadings of the first three principal components extracted from 118 log-transformed skull measurements.
Figure S1. Illustration of the locations of the CMs (craniodental measurements) used in the present study.
Figure S2. Phylogeny of the NFSC reconstructed by using IRBP. Posterior probabilities from Bayesian analyses in MrBayes and bootstrap values from maximum likelihood analyses in IQ-TREE are given as node labels.
Figure S3. Species delimitation of the NFSC by using the GMYC, PTP and MPTP methods.
Figure S4. Skin and skull specimens of holotypes examined in the present study. A, *Niviventer fulvescens*, NHM. 4.5.18.377. B, C, *Niviventer mekongis*, NHM 7172/H (26.11.16.13), HBL = 136. Left in D, E and F,G, *Niviventer huang*, NHM 98.11.1.16, HBL = 155, TCL = 36.20. Right in D, E and H, I, *Niviventer ling*, NHM 98.3.7.8, HBL = 132, TCL = 32.52.